ON THE FORCHHEIMER COEFFICIENTS FOR UNSATURATED FLOWS

Anton Ali[1]* and Deborah Villarroel-Lamb[2]

[1,2]Faculty of Engineering, The University of the West Indies, Trinidad
[1]Email: anton_1991@live.com*
[2]Email: deborah.villarroel-lamb@sta.uwi.edu

Abstract: The Darcy- Forchheimer equation is the most common model used in describing porous media flow. Many CFD pre-packaged platforms offer this model via the modified Navier- Stokes equations and typically implement the model under a penalization scheme. Although the theoretical basis of the Darcy-Forchheimer equation is unquestionable, its use is dependent on introduced coefficients which vary with practical applications. Despite a general range of values, the selection of these coefficients is somewhat subjective in saturated cases. For transient unsaturated flow cases, the selection of these coefficients may even be further complicated. This research experimentally investigated the inherent nature of these Darcy-Forchheimer coefficients for unsaturated flows in naturally occurring porous media. The results suggest variability of these coefficients with the transient nature of this flow regime. Thus, highlighting the invalidity of a single combination of coefficients across the entirety of unsaturated flows in natural porous media.

Keywords: *Darcy- Forchheimer coefficients, Natural porous media, Unsaturated flows.*

1.   Introduction

Porous materials can be found almost everywhere in both the manmade and natural environment. Indeed, all materials have varying degrees of porosity, the only exceptions may be considered as either being metals, plastics and extremely dense materials. Coupled with the well-known fact that 70% of the earth surface is covered by water, porous media flow has attracted much attention from a historical context. In general, these flows can be divided into several subdivisions; unsaturated or saturated, steady or unsteady as well as linear or non-linear. Of these, many researchers have devoted significant efforts to better understand and reveal the processes for the saturated case.

For saturated- steady flows, at a macroscale, earliest works can be dated to Henry Darcy 1865 for the linear subdivision whilst the nonlinear case was developed by Phillip Forchheimer (1901); the results are the well-known Darcy and Forchheimer equations respectfully. Both equations have been successfully applied with the use of empirical coefficients which vary with porous media. However, it should be noted that in the absence of experimental determination, the Forchheimer introduced coefficient is less well universally described by universal models [1].

For saturated-unsteady cases, modifications to the Darcy's and Forchheimer's law have been developed by the addition of an acceleration term for both linear and non-linear cases. An empirical coefficient is also applied to this added acceleration term and is typically found via empirically based predictive models. Despite reasonable applications of both the modified Darcy's and

Forchheimer's laws, a single combination of the inherent empirical coefficients evident from the steady case as well as the added empirical coefficient for the unsteady modified term, may not be valid over the entirety of a transient saturated problem [2]. Zhu (2016),([3]), highlighted this for nonlinear cases where a sudden step change in pressure gradient is evident. Thus, the application of the modified Forchheimer's Laws for saturated unsteady non-linear flows are complex due to the transient nature of the empirical coefficients evident in such cases.

Unsaturated porous flows are generally modelled by the modified Forchheimer's law can be readily applied. Its application, already complex for saturated case, may be further exacerbated due to a differing nature of coefficients variability as media water content varies for these flows. Moreover, depending on the media characteristic pore size and material constitution, the effects of negative suction pressure may become noticeable. Undoubtedly, the application of the modified Forchheimer's law for describing unsaturated flows are uncertain and multiplex. Despite this, a few researchers (e.g. [4] and [5]) have had relative success in applying the modified Forchheimer's equation to such cases. It should be noted however, this was generally achieved via numerical experimentation which involved varying a single combination of the Forchheimer's coefficients which best described the problem at hand.

This paper seeks to investigate the nature of the Forchheimer's coefficients for unsaturated flows in natural homogenous porous media. More specifically, the authors attempt to ascertain the validity of utilizing a single combination of coefficients over the entirety of an unsaturated flow problem, as well as the significance of each component of the Forchheimer's equation for such flows. Section 2 gives the theoretical background and equations typically used in describing porous media flow. Section 3 outlines the experimental set-up & method used to investigate the coefficients for unsaturated cases. Section 4 provides the results obtained and analysis of observable trends. Finally, Section 5 provides concluding remarks.

2. Background and Theory

The Darcy's law, Eq. (1), was obtained in 1865 upon an experimental basis for saturated-steady-linear porous media flows at very low pore Reynolds numbers (Re_p) given by Eq. (2). In such flows viscous forces dominate, hence Eq. (1) utilizes this basis in outlining a linear relation between the average porous media flow velocity (U_p) and the driving pressure difference (∇P) across the media. The law employs a permeability coefficient (K) which varies with porous media and may range from O(h)= 10^{-5} m^2 to 10^{-20} m^2 depending on the media in question [6]

$$\nabla P = - \frac{\mu}{K} \cdot U_p \tag{1}$$

$$Re_p = \frac{\rho \, U_p \, \delta}{\mu} \tag{2}$$

Where μ is the dynamic viscosity, ρ is the density of the fluid flowing through the porous media and δ is the characteristic pore size of the media. As infiltration velocity increases, contributions due to inertial effects become evident and the transition from saturated- steady-linear to saturated-steady-nonlinear flows occur. In general, Eq. (1) is valid for $Re_p < 1$[7] whilst the transition between the mentioned occurs in the range $1 < Re_p < 10$ [6]. For saturated-steady porous media flows beyond $Re_p = 10$, the Forchheimer equation, Eq. (3), becomes valid where a quadratic velocity term is added to account for any momentum imbalance attributed to inertial effects.

$$\nabla P = - {}^{\mu}\!/_{K} \cdot U_p \ - \beta \cdot \rho \cdot U_p |U_p| \tag{3}$$

Where β is the Forchheimer's coefficient.

For saturated-unsteady flows, a phase shift between ∇P and U_p can exist [8]. Modifications of Eq. (1) and Eq. (2) via an added time derivative of U_p term is introduced to account for this occurrence, yielding the unsteady Darcy equation, Eq. (4), and unsteady Forchheimer equation, Eq. (5), respectfully.

$$\nabla P = - {}^{\mu}\!/_{K} \cdot U_p \ - c \cdot {}^{\partial(U_p)}\!/_{\partial t} \tag{4}$$

$$\nabla P = - \frac{\mu}{K} \cdot U_p \ - \beta \cdot \rho \cdot U_p |U_p| \ - c \cdot {}^{\partial(U_p)}\!/_{\partial t} \tag{5}$$

Where c is an inertia coefficient factored to the acceleration term. For saturated-unsteady cases, an assumption of constant K and β equivalent to their saturated-steady values is commonly made. The coefficient c however, has proven to be more challenging where no consensus on a standardized expression across all porous media has yet been achieved. Furthermore, it is still unclear whether a single combination of K, β and c is capable of describing saturated-unsteady and non-linear flows to an acceptable degree [3].

Unsaturated porous flows, are unsteady and non-linear, thus highlighting Eq. (5) in such cases. However, the uncertainties of K, β and c becomes further compounded for such flows. Further, depending on the porous medium, the effects of an additional suction pressure may become significant. The Richard's equation, Eq. (6) – (vector differential form), describes the movement of water for such flows and accounts for this additional pressure along with its variation with the transient water content of the media.

$$\rho \cdot {}^{\partial \theta}\!/_{\partial t} = \nabla \cdot \left[K_h(\psi_m)(\nabla \psi_m + g \, \widehat{Z}) \right] \tag{6}$$

Where θ is the volumetric water content of the media, ψ_m is the matric potential, $K_h(\psi_m)$ is the hydraulic conductivity of the media at matric potential ψ_m, g is acceleration due to gravity and $\widehat{Z}$ is the unit vector in the vertical direction. Equation (6) is qualitatively consistent with predictions from Eq. (1) [9], and typically used for transient soil-based processes such as infiltration and evaporation. It should be noted that negative suction pressures are generally associated with fine grain soils where flows do not transition beyond the viscous dominated regime. Nonetheless, a combined generic equation for unsaturated porous flows is proposed via Eq. (7) where respective terms may become invalid depending on the flow scenario and media.

$$\left[\nabla \psi_m + g \, \widehat{Z} + \nabla \psi_e \right] = \ A_1 \cdot U_p + B_2 \cdot U_p |U_p| + C_3 \cdot {}^{\partial(U_p)}\!/_{\partial t} \tag{7}$$

Where the ensembled contributions due to the Forchheimer coefficients are: A_1 (units: t^{-1}), B_2 (units: t/L) and C_3 (dimensionless), ψ_e is an acceleration due to an externally applied potential. It should be noted all terms on the left-hand side of Eq. (7) are expressed in terms of an acceleration.

3.   Experimental Set-up and Data Processing

Investigating unsaturated porous media flow problems are rare. Consequently, with the exception of matric suction apparatus, no general specialized equipment exists for such flows. Resultantly, experiments were developed which would allow some degree of control whilst permitting the measurement of key variables as flow developed.

The experiments were carried out in the Soils Laboratory of the Civil & Environmental Engineering Department at the University of the West Indies, St. Augustine Campus. A transparent vertical square column of side width 0.1m and length 0.5m open at one end and fitted with a wire mesh at other was used as shown in Fig. 1. The column was partitioned with a removable water tight gate midway of the channel length which separated the column into two sections. The lower section was completely filled with dry homogenous coarse grain material and kept in place by the fitted wire mesh. The above section was filled to a desired water depth and prevented from entering the porous media by the removable gate.
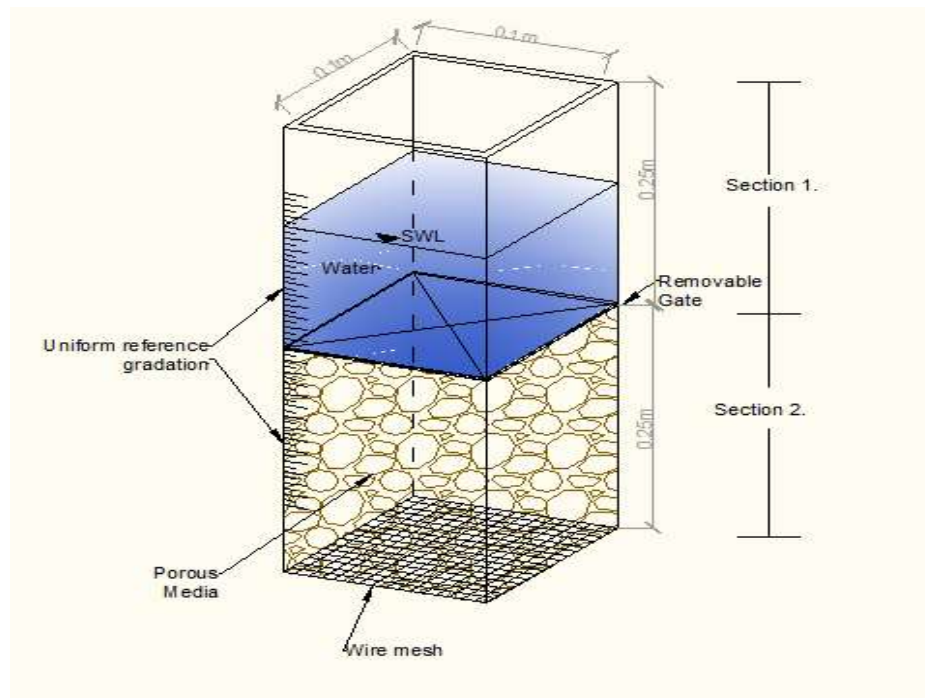

Figure 1: Laboratory experiment set-up

The experiments involved removing the gate at high speed, thereby allowing the above water to infiltrate into the unsaturated porous media. High frame rate videos were taken along the transparent walls of the column and specifically monitored the water front progression through the porous media as well as the progressive decrease of the water depth elevation in the above section. Video observations were referenced against 0.0025m gradations in the direction of flow which was zeroed at the gate location. The experiments were carried out for four different natural

homogenous porous media with properties as outlined in Table.1, each at 25 different initial infiltrating water depths ranging from 0.03-0.2m.

Table. 1: Porous media and properties used in experiment

Porous media	Size Range (mm)	D_{50} (mm)	Porosity	Classification	Saturated Hydraulic Conductivity/K_h (cm/s)
A	4.75-2.36	3.40	0.487	fine-very fine pebbles	3.75
B	2.00-1.40	1.75	0.425	very coarse sand	1.63
C	1.40-1.00	1.20	0.369	very coarse – coarse sand	1.13
D	0.85-0.71	0.80	0.309	coarse sand	0.75

Time referenced images were extracted from video observations at a frequency of 20Hz. Both the temporal progression of the infiltrating water front (within the porous media) and the decreasing Still Water Line (SWL) level (in the reservoir above) were used to calculate the instantaneous depth-averaged flow velocity of the media (U_p). This was accomplished via visually observing the location change of each water front with time, thus yielding the exact velocity at these locations. A weighted averaging, zero-referenced at the gate location as outlined in Fig. 2 and computed via Eq. (8), was then used to acquire U_p for the corresponding infiltrated water depth (D_{Inf}) and pressure head (H).
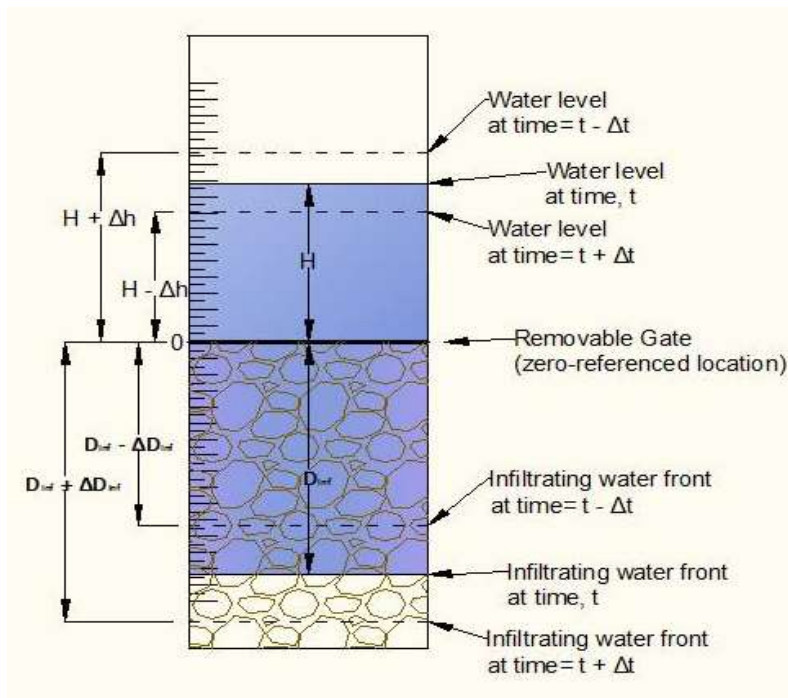
Figure 2: Measurements used in calculation of U_p

$$U_p(H, D_{Inf}) =$$

$$\left[\left(\frac{(H+\Delta h)-(H-\Delta h)}{(t+\Delta t) - (t-\Delta t)} \right) \cdot D_{Inf} + \left(\frac{(D_{Inf}+\Delta D_{Inf})-(D_{Inf} - \Delta D_{Inf})}{(t+\Delta t) - (t - \Delta t)} \right) \cdot H \right] \Bigg/ (D_{Inf} + H)$$

(8)

The temporal variation of U_p is dependent on both D_{Inf} and H. Thus, the acceleration term in Eq. (7) is also dependent upon these values. Utilizing computed values of U_p at various H and D_{Inf} combinations, the acceleration term in Eq. (7) was then obtained via a simple central differencing of Up given by Eq. (9).

$$\partial U_p(H, D_{Inf}) \Big/ \partial t = \left[U_p(H - \Delta h, D_{Inf} + \Delta D_{Inf}) - U_p(H+\Delta h, D_{Inf} - \Delta D_{Inf}) \right] \Big/ 2\Delta t$$

(9)

Where: $U_p(H - \Delta h, D_{Inf} + \Delta D_{Inf})$ is the instantaneous depth-averaged porous media velocity for pressure head: $H - \Delta h$ and infiltrated depth: $D_{Inf} + \Delta D_{Inf}$ occurring at time: $t+\Delta t$. Similarly, $U_p(H + \Delta h, D_{Inf} - \Delta D_{Inf})$ is the instantaneous depth-averaged porous media velocity for pressure head: $H + \Delta h$ and infiltrated depth: $D_{Inf} - \Delta D_{Inf}$ occurring at time: $t - \Delta t$.

Assuming negligible suction pressure due to the coarse-grained composition of the porous media ($\psi_m=0$), all but the coefficients in Eq. (7) were obtained. An analysis of the Forchheimer's coefficients via substitution of known values of U_p, flow acceleration and pressure head into Eq. (7) was then pursued. Differing combinations of corresponding U_p, flow acceleration and pressure head were used to yielding a solvable linear system of equations from Eq. (7). As a result of the three coefficient unknowns (A_1, B_2 and C_3), a selection of three combinations of these values were needed. The experimental methodology outlined was subjected to a few limitations. The most critical of these were due to the non-instantaneous removal of the gate, surface tension effects between the fluid and the walls of the column as well as any non-uniformity within the media which may have affected local porosity and thus flow. Hence, the results obtained would reflect the cumulative effect of these constraints which emanate from the experimental procedure.

4.   Results and Analysis

The results outlined velocity observations qualitatively similar to those expected from Eq. (1) and Eq. (3) – Eq. (7) where a general power law profile is observed when varying U_p with D_{Inf}. Moreover, consistent with popular infiltration models, the results outlined a tendency of U_p to converge to the saturated K_h values as D_{Inf} increased, irrespective of the driving pressure head. Characteristic plots are provided in Fig. 3.

Direct representative results for porous media B and D are provided in Table. 2 – section A and Table. 3 – section A respectively. The results provide computed U_p and flow acceleration values for 12 ψ_e pressures across 3 D_{Inf} values for each media. Section B of Table. 2 and Table. 3 presents computed A_1, B_2 and C_3 ensembled coefficient values obtained via linear systems from Eq. (7) and the values presented in Section A of the relevant tables. Section B of both tables highlight the sensitivity of the Forchheimer's coefficients to both the instantaneous driving pressure head and D_{Inf}. At a constant D_{Inf} value, differing driving pressures yielded different linear systems, which when resolved resulted in varying coefficient values. Similar observations were noted for converse systems where ψ_e was held constant and D_{Inf} varied.

Negative coefficient values were also observed across most cases. These values are considered unrealistic since they factor each term on the right-hand side of either Eq. (7), each of which addresses different aspects in porous media flows. These overall factored terms should not contradict nor subtract from each other, but rather become active and add to the shortcomings of previous terms, hence highlighting a negative combination as unrealistic. Moreover, such values are deemed to be the result of two main effects: (1) Inaccuracies in computing U_p due to the visual method adopted. (2) The result of solving the linear system mathematically without imposing any realistic bounds upon A_1, B_2 and C_3.
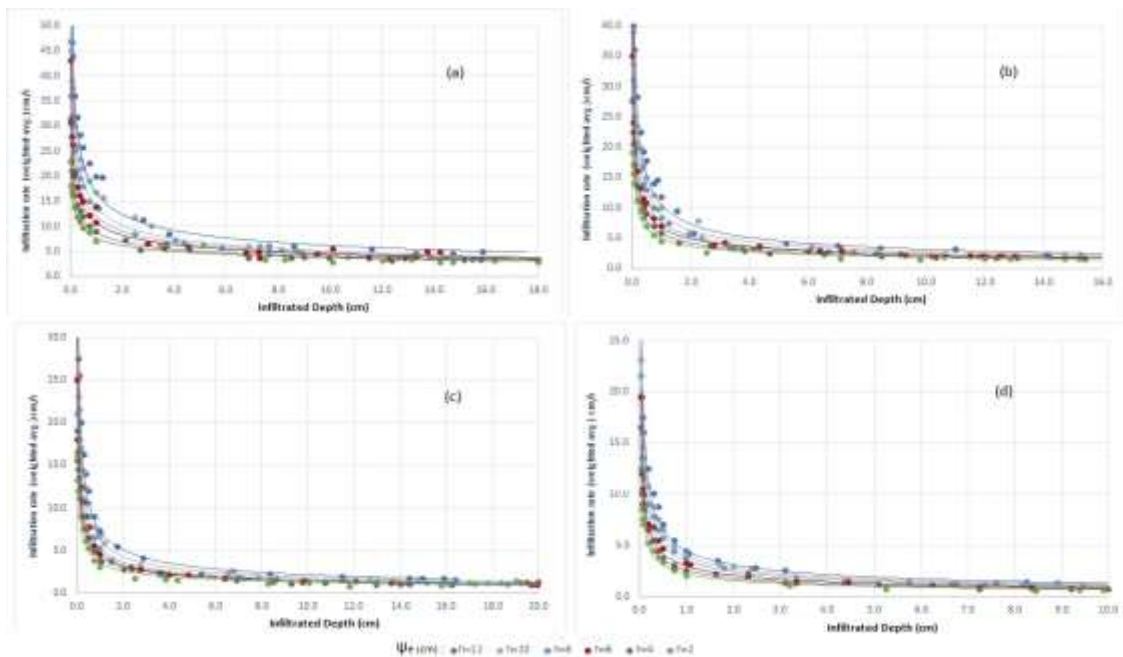
Figure 3: (a) Porous media A - U_p variation with Infiltrated depth for ψ_e ranging 2-12 cm (b) Porous media B - U_p variation with Infiltrated depth for ψ_e ranging 2-12 cm (c) Porous media C - U_p variation with Infiltrated depth for ψ_e ranging 2-12 cm (d) Porous media D - U_p variation with Infiltrated depth for ψ_e ranging 2-12 cm

Noting error mitigation could not be improved due to the experimental methodology, only an analysis with assumed bounded coefficient values could be pursued. Firstly, the ensembled A_1 coefficient is directly related to the hydraulic conductivity (K_h) of the porous media. K_h is

understood as constant value for a fully saturated media. However, for coarse-grained materials, K_h values may differ between the saturated and unsaturated case [9]. Nonetheless, a constant A_1, equivalent to the saturated value outlined in Table. 1, is assumed valid for the unsaturated regime. Secondly, due to the high porosity of each media used in the experiments, coupled with the smooth variation of ψ_e as water infiltrated each media, the occurrence of any phase-lag between ψ_e change and U_p can be assumed negligible. Thus, the C_3 coefficient is assumed to be zero ($C_3=0$). Resultantly, Equation (7) simplifies to an analysis of B_2 under such assumptions, resolvable by any single combination of ψ_e and U_p in Section A of Table. 2 and Table. 3, without the need for a linear system. The computations for which are presented in Section C of the respective tables.

A comparison between the ensembled coefficients in Sections B and C of Tables. 2 and 3 highlight positive and more realistic values as a result of the assumptions made. Therefore, as is evident in saturated applications, coefficient values must be directly linked and hence bounded to some physical basis and not selected solely upon best fit numerical experimentation. Despite improved results, Section C of both Tables. 2 and 3 highlight the high variability of B_2 as both ψ_e and D_{Inf} varied. For all media, variations ranged over $O(h)=10^1$ where no general variation trend was observed. Hence, for the simplifying assumptions made, it can be stated that a constant value of the B_2 coefficient is invalid for the entirety of unsaturated coarse-grained flows.

Table 2: Experimental results and computed Forchheimer coefficients for porous media B

Section A					Section B				Section C		
D_{Inf} (cm)	ψe (cm)	U_p (cm/s)	$\frac{\partial(U_p)}{\partial t}$ (cm/s^2)	Case No.	A_1 (s^{-1})	B_2 (sm^{-1})	C_3	Cases used	A_1 (s^{-1})	B_2 (sm^{-1})	C_3
2	3.75	4.09	-19.7	1	715.29	-722.38	-609.38	2,3,4	594.30	23.44	0
	3.90	4.13	-20.11	2	739.75	-741.77	-620.79	1,3,4	594.30	26.18	0
	4.00	4.15	-20.39	3	803.53	-788.97	-647.71	1,2,3	594.30	27.92	0
	4.25	4.21	-21.12	4	757.01	-754.97	-628.44	1,2,4	594.30	32.01	0
	7.75	5.36	-34.84	5	362.82	-143.52	-199.74	6,7,8	594.30	55.85	0
	7.90	5.42	-35.57	6	359.38	-145.82	-202.16	5,7,8	594.30	55.84	0
	8.00	5.46	-36.07	7	352.62	-151.33	-207.75	5,6,7	594.30	55.81	0
	8.25	5.57	-37.33	8	357.27	-147.37	-203.77	5,6,8	594.30	55.62	0
	11.75	7.36	-58.51	9	707.05	-49.97	-72.54	10,11,12	594.30	43.99	0
	11.90	7.45	-59.56	10	702.14	-50.53	-73.67	9,11,12	594.30	43.32	0
	12.00	7.51	-60.27	11	691.32	-51.87	-76.27	9,10,11	594.30	42.87	0
	12.25	7.66	-62.07	12	698.95	-50.91	-74.42	9,10,12	594.30	41.73	0
5	3.75	2.83	-3.99	13	-550.78	742.50	669.07	14,15,16	594.30	5.01	0
	3.90	2.85	-4.07	14	-541.85	734.13	658.59	13,15,16	594.30	6.82	0
	4.00	2.87	-4.13	15	-523.90	716.53	636.01	13,14,15	594.30	7.98	0
	4.25	2.91	-4.28	16	-536.33	728.83	651.88	13,14,16	594.30	10.74	0

7.75	3.54	-7.15	17	2012.83	-1190.67	-1439.07	18,19,20	594.30	32.21	0
7.90	3.57	-7.31	18	2090.04	-1253.21	-1510.40	17,19,20	594.30	32.59	0
8.00	3.59	-7.41	19	2298.98	-1421.10	-1701.07	17,18,19	594.30	32.83	0
8.25	3.64	-7.68	20	2145.35	-1297.83	-1561.18	17,18,20	594.30	33.36	0
11.75	4.42	-12.15	21	835.55	-176.24	-249.56	22,23,24	594.30	34.27	0
11.90	4.45	-12.37	22	837.59	-178.83	-252.97	21,23,24	594.30	34.12	0
12.00	4.48	-12.52	23	842.73	-185.00	-261.01	21,22,23	594.30	34.01	0
12.25	4.54	-12.9	24	839.00	-180.57	-255.25	21,22,24	594.30	33.73	0
3.75	1.84	-0.58	25	2277.84	-933.12	-540.49	26,27,28	594.30	76.72	0
3.90	1.84	-0.61	26	2282.69	-935.85	-540.97	25,27,28	594.30	80.70	0
4.00	1.84	-0.63	27	2293.37	-941.76	-541.57	25,26,27	594.30	83.22	0
4.25	1.85	-0.69	28	2285.84	-937.60	-541.21	25,26,28	594.30	89.06	0
7.75	2.16	-2.01	29	1231.54	-269.74	-168.27	30,31,32	594.30	97.96	0
7.90	2.19	-2.09	30	1238.19	-275.11	-173.61	29,31,32	594.30	95.95	0
8.00	2.2	-2.15	31	1255.08	-288.12	-185.70	29,30,31	594.30	94.56	0
8.25	2.25	-2.28	32	1242.83	-278.76	-177.11	29,30,32	594.30	90.87	0
11.75	3.09	-4.75	33	1099.71	-70.74	123.87	34,35,36	594.30	31.83	0
11.90	3.13	-4.88	34	1098.57	-71.72	121.16	33,35,36	594.30	29.60	0
12.00	3.17	-4.96	35	1096.45	-74.08	115.04	33,34,35	594.30	28.15	0
12.25	3.25	-5.18	36	1097.88	-72.38	119.38	33,34,36	594.30	24.61	0

(Note: rows 25–36 belong to D_{Inf} = 10)

Table 3: Experimental results and computed Forchheimer coefficients for porous media D

	Section A				Section B				Section C		
D_{Inf} (cm)	ψe (cm)	U_p (cm/s)	$\frac{\partial(U_p)}{\partial t}$ (cm/s²)	Case No.	A_1 (s⁻¹)	B_2 (sm⁻¹)	C_3	Cases used	A_1 (s⁻¹)	B_2 (sm⁻¹)	C_3
2	3.75	1.77	-3.30	37	161.63	1128.25	307.13	38,39,40	1307.47	161.59	0
	3.90	1.80	-3.41	38	158.96	1133.71	310.89	37,39,40	1307.47	169.39	0
	4.00	1.82	-3.49	39	153.88	1145.59	319.48	37,38,39	1307.47	174.35	0
	4.25	1.86	-3.69	40	157.35	1137.23	313.37	37,38,40	1307.47	185.96	0
	7.75	2.42	-7.34	41	517.55	698.04	75.17	42,43,44	1307.47	278.53	0
	7.90	2.44	-7.54	42	512.13	702.82	77.19	41,43,44	1307.47	280.81	0
	8.00	2.46	-7.67	43	500.11	713.71	81.90	41,42,43	1307.47	282.29	0
	8.25	2.49	-8.01	44	508.60	705.97	78.54	41,42,44	1307.47	285.84	0
	11.75	2.98	-13.63	45	900.75	412.95	-28.72	46,47,48	1307.47	321.84	0
	11.90	3.00	-13.90	46	896.52	415.57	-27.94	45,47,48	1307.47	323.04	0

	12.00	3.01	-14.09	47	886.95	421.62	-26.09	45,46,47	1307.47	323.83	0
	12.25	3.04	-14.57	48	893.75	417.31	-27.42	45,46,48	1307.47	325.78	0
5	3.75	1.10	-0.39	49	203.08	1584.98	1104.99	50,51,52	1307.47	232.93	0
	3.90	1.11	-0.40	50	206.30	1578.78	1094.66	49,51,52	1307.47	240.87	0
	4.00	1.12	-0.40	51	210.83	1567.55	1072.31	49,50,51	1307.47	245.80	0
	4.25	1.14	-0.42	52	208.00	1575.12	1088.03	49,50,52	1307.47	256.89	0
	7.75	1.46	-1.00	53	10317.80	-10325.1	-9399.68	54,55,56	1307.47	281.57	0
	7.90	1.48	-1.04	54	12290.89	-12688.3	-11545.1	53,55,56	1307.47	279.13	0
	8.00	1.49	-1.07	55	23117.26	-25634.0	-23273.3	53,54,55	1307.47	277.42	0
	8.25	1.51	-1.13	56	14138.38	-14899.2	-13550.1	53,54,56	1307.47	272.84	0
	11.75	1.96	-2.37	57	2137.52	-386.94	-244.33	58,59,60	1307.47	187.74	0
	11.90	1.99	-2.44	58	2141.92	-394.12	-252.36	57,59,60	1307.47	183.88	0
	12.00	2.00	-2.48	59	2152.91	-411.34	-271.27	57,58,59	1307.47	181.32	0
	12.25	2.04	-2.59	60	2144.95	-398.97	-257.74	57,58,60	1307.47	174.96	0
10	3.75	0.88	0.00	61	1491.28	50.40	0.00	62,63,64	1307.47	263.97	0
	3.90	0.89	0.00	62	1483.37	59.24	0.00	61,63,64	1307.47	261.90	0
	4.00	0.89	0.00	63	1478.16	65.18	0.00	61,62,63	1307.47	260.44	0
	4.25	0.91	-0.02	64	1495.99	44.88	0.00	61,62,64	1307.47	256.48	0
	7.75	1.15	-0.13	65	-500.91	2304.20	5806.24	66,67,68	1307.47	177.91	0
	7.90	1.17	-0.14	66	-320.52	2102.73	5340.30	65,67,68	1307.47	174.19	0
	8.00	1.17	-0.14	67	-14.31	1760.45	4546.42	65,66,67	1307.47	171.72	0
	8.25	1.19	-0.15	68	-219.20	1989.52	5078.10	65,66,68	1307.47	165.55	0
	11.75	1.49	-0.38	69	1767.74	-212.94	74.30	70,71,72	1307.47	85.92	0
	11.90	1.50	-0.39	70	1771.32	-217.15	63.73	69,71,72	1307.47	82.91	0
	12.00	1.51	-0.40	71	1780.04	-227.32	38.46	69,70,71	1307.47	80.92	0
	12.25	1.54	-0.42	72	1773.76	-220.01	56.60	69,70,72	1307.47	76.02	0

In real life situations a constant K_h value is invalid for the entirety of unsaturated flows, outlining the variability of A_1 for such cases. Noting the results of Section C which outlined the variability of B_2 for a constant A_1, further variation of B_2 is foreseen in cases where A1 is also allowed to vary. Thus, further confirming the invalidity of a constant B_2 for unsaturated porous flows. Although A_1 may tend to some constant value as D_{Inf} increases, a similar trend may not be observed for B_2 as the results of Section C for both media show a dependence of B_2 on ψ_e and D_{inf}. Unlike A_1 and B_2, no meaningful analysis of the C_3 coefficient for unsaturated flows can be made. This coefficient is the most complex and least understood of the Darcy-Forchheimer coefficients, much ambiguity surrounds the nature of this coefficient for saturated unsteady cases [3], thus its effect in unsaturated flows are further complex and subject of further research.

Noting the mentioned, it can be stated that a single combination of A_1, B_2 and C_3 is invalid over the entirety of the unsaturated flow regime. Moreover, even for cases where arguable assumptions on constant A_1 and C_3 can be made, the variability of B_2 is evident. Finally, the results also confirm

the theoretical structure of Eq. (7) where flow acceleration and velocity values increase with increasing ψ_e, whilst an inverse relation exist between both values and D_{inf}.

5.   Conclusion

The Darcy-Forchheimer's equation is well known to be the current state of the art in modelling saturated-unsteady porous media flows. Despite relatively successful applications to unsaturated flows, much ambiguity surrounds the empirical coefficients employed within for such cases. This paper examined the nature of these coefficients for such cases via one-dimensional laboratory flow experiments on coarse-grained media. The analyzed results underlined the need for realistic bounds in the selection of coefficient values for such flows. For cases where simplifying assumptions of a constant linear coefficient and zero acceleration coefficient were made, a high variability of the quadratic coefficient with pressure head and infiltrated depth was observed. Suggesting that for real-life application where such assumptions are not suitable, even greater variability of this coefficient can be expected. Unfortunately, no clear-cut relationship was observed across any of the coefficients, neither was there any meaningful evaluation regarding the significance of each term comprising the Darcy-Forchheimer equation. However, it is unquestionably evident that a single combination of the unsteady Darcy-Forchheimer's coefficients is invalid over the entire range of unsaturated coarse-grained porous media flows.

References

[1] W. Sobieski, A. Trykozko. Sensitivity Aspects of Forchheimer's Approximation. *Transport in Porous Media* 89, (2011) 155-164.

[2] H. F. Burcharth, O. K. On the one-dimensional steady and unsteady porous flow equations. *Coastal Engineering* 24 no. 3-4, (1995) 233-257.

[3] T. Zhu. Unsteady porous-media flows. *Ph.D. Thesis, Technische Universität München,* (2016).

[4] J. C. Pintado-Patiño, A. Torres-Freyermuth, J. A. Puleo, D. Pokrajac. On the role of infiltration and exfiltration in swash zone boundary layer dynamics. *Journal of Geophysical Research: Oceans* 120 no. 9, (2015) 6329-6350.

[5] A. M. Hammeken, R. R. Simons. 2017. Numerical study on the influence of infiltration on swash hydrodynamics and sediment transport in the swash zone. In *Coastal Engineering Proceedings*, *1*(35), *currents.3.* Antalya. Turkey.

[6] F. Cimolin, M. Discacciati. Navier–Stokes/Forchheimer models for filtration through porous media *Applied Numerical Mathematics* 72, (2013) 205-224.

[7] G. S. Beavers, D. D. Joseph. Boundary conditions at a naturally permeable wall. *Journal of Fluid Mechanics* 30 no. 1, (1967) 197-207.

[8] M. Laushey, L. V. Popat. (1967). Darcy's law during unsteady flow. In *Ground water: General assembly of Bern* 77, 284–299.

[9] M. Bittelli, G. S. Campbell, F. Tomei. 2015. *Soil Physics with Python: Transport in the Soil–Plant–Atmosphere System.* Oxford University Press.